An Investigation of Tin Whisker Growth over a 32 Year Period

M.A. Ashworth [1] and B. Dunn [2]

[1] Department of Materials, Loughborough University, Loughborough, Leicestershire, LE11 3TU, UK

[2] School of Engineering, University of Portsmouth, UK

Corresponding author:

Email: m.a.ashworth@lboro.ac.uk,

Tel: +44 (0)1509 225406

Abstract

This paper presents the results of a 32 year old laboratory study of whisker growth from tin electrodeposits. The study was originally undertaken to gain an increased understanding of the phenomenon of tin whisker growth with respect to: substrate material (brass and steel), the influence of a copper-plated barrier layer, the nature of the electroplated tin utilised (normal, abnormal or contaminated), post-electrodeposition fusing of the tin and stress level applied to the specimens. Whisker growth was evaluated using electroplated C-rings (both stressed and un-stressed) that were stored throughout in a desiccator at room temperature.

Whisker growth for the samples was first reported after 3½ years storage in September 1987 (ESA STR-223 report, *'A laboratory study of tin whisker growth'*) [1]. An updated analysis of whisker growth was subsequently reported in March 2006 (ESTEC Materials Report 4562, *'15½ years of tin whisker growth'*) [2]. Further analysis of whisker growth has recently been undertaken to evaluate whisker growth after 32 years storage. SEM analysis has been undertaken to investigate whisker length and, using polished cross-sections, the morphology, thickness and type of intermetallic formation. The properties of such whiskers will be described. Subsequently an account of how tin whiskers have grown on C-ring samples that were carefully stored under dry, ambient conditions will be given. The 'incubation periods' from electroplating the tin, until the emergence of whisker growths are fascinating.

Knowledge about vintage whiskers is important in order that we can take steps to increase the resiliency of our space missions. Similarly, such knowledge is important to engineers engaged on products reaching their nominal end-of-life, but where for reasons of economy, these products cannot be replaced. We rely on a wide range of 'older' electronic products that serve our domestic utilities as well as our space, communications, military and entertainment industries.

1. Introduction

Work concerning the characterisation of tin whiskers was initiated at the European Space Agency (ESA) in the mid-1970's [3] but it was not until 1982 that a more rigorous study of whiskers was undertaken as, in this period, a spacecraft electronic circuit was seen to malfunction and tin whiskers were considered to have been a potential cause of short circuiting. The relationship between tin whisker diameter and the applied current needed to cause whisker burn-out was calculated from actual measurements in the laboratory – the vexing problem of short circuiting was also identified when currents could flow through whiskers without burn-out, as shown in Figure 1 [4]. Unwanted growths of tin whiskers are known to severely jeopardise the reliability of electronic circuits. This is particularly true when the whiskers grow to long lengths in the order of 1 to 2 mm and produce electrical short circuits in low voltage equipment. Between 1972 and 1985 laboratory findings at ESA revealed several tin whisker issues on space hardware, tin whiskers were growing from: tin-plated terminal pins designed for soldering (Sn on Cu on brass); a tin plated housing; plated through holes on a pure tin finished printed circuit board; tin plated lugs for crimping and soldering; tin-plated steel springs and contact points on electrical switches; and, vacuum deposited tin on the inside of a plastic back-shell connector protector [5]. In 1985 pure tin was prohibited by the contractual requirements of the ESA standards covering the selection of materials for space use and the top level electronic component procurement standards. Tin-lead solder alloys and tin-lead solderable finishes were recommended and space-qualified for ESA electronic systems as it was known that the addition of at least 3% lead to pure tin, was a reliable mitigation against whisker growth (see for instance ECSS-Q-ST-70-08 [6]). From the mid-80's until the mid-10's, with two notable exceptions, no whisker anomalies have been reported on ESA projects.

Sweeping changes to the electronics manufacturing industry were introduced by the European Parliament and Council in 2006 [7]. The EU directives such as RoHS now specifically forbid the traditional use of lead in the composition of the components, circuit boards and solders used in the assembly of electronic circuits. Commercial electronic

equipment should now contain no lead. Although the space, aircraft and medical sectors are presently exempt from the lead-free rules, lead-free items (mainly components having pure tin plated terminations) destined for the vast commercial markets, have also infiltrated the "exempt" high reliability industries. Tin whiskers and the problems they cause have now returned to the stage and hence there is again a need to understand how they grow, how they can create electrical and mechanical failures and particularly, what means can be used to mitigate against their growth.

Financial constraints now necessitate that both professional and commercial electronic systems such as motor vehicles, televisions, computer hardware and the like, incorporate the philosophy of redundant circuits and throw-away modules. This means it is unlikely that any failure analysis will be performed on defective hardware and it appears likely that rejected modules will support ubiquitous colonies of microscopic whiskers that will never be detected during any post-mortem by the 'forensic scientist'.

The laboratory study of tin whisker growth [1] using so-called 'C-ring samples' has been on-going since the samples were manufactured in 1982. This is probably one of the longest whisker study to have been undertaken under strict conditions of isothermal ageing in a non-corrosive environment. An updated analysis of whisker growth was subsequently reported in March 2006 (ESTEC Materials Report 4562, *'15½ years of tin whisker growth'*). In this present paper we have re-examined the length of whiskers present on the C-rings after 32 years storage. Metallographic work has now been performed to reveal the microstructure and the growth of intermetallic compounds (IMC) at the various plating-to substrate interfaces.

2. Experimental procedures

2.1 The Test Specimens, their plated layers and method of stressing

The original report [1] can be consulted for a detailed description of the test specimen. The samples consisted essentially of machined C-rings having the dimensions shown in Figure 2.

Stress can be applied to these rings by tightening the nuts on the bolt; this is rather similar to C-rings designed for stress corrosion testing (ASTM, 2013) [8]. The rings were manufactured to represent certain spacecraft electronic systems utilised in the 1970's, but which may also represent unapproved or counterfeit components assembled into today's electronic circuits. The base metals were steel and brass, with and without a nominally 3 μm copper barrier layer (occasionally seen to be actually 1.5 or 2 μm).

The final finish was pure, electroplated "normal" tin as used commercially. For some samples the normal tin was fused in a controlled, non-oxidising atmosphere. Two additional variants for the tin plating were designed into the study:

"Abnormal" tin to represent a plating bath depleted in tin and operated at a high current density to provide a deposit with compressive stress, and

"Contaminated" bath to represent an electrolyte containing organic contamination (flour dust was used to plate-in occlusions and filtration was not applied to this bath).

The plating bath conditions are recorded in Table 1. Three samples of every test variant were produced.

Tin whisker growths were thought to result from the application of compressive stress to the plated finish. The C-rings were loaded and this caused them to deflect – the compressive test stresses applied to the various tin platings were:

None, 'slight' (50 MPa) and 'high' (400 MPa).

It will be noted from Figure 2 that these maximum test stresses are applied at 90^{o} to the C-ring axis, so that sin α= 1. There will be a progressive reduction in resultant stress along each quadrant as the factor of sin α tends to zero. Conversely, as the C-rings are loaded their outer surface will be subjected to a range of tensile stresses.

2.2 Storage Conditions

The specimens (40 in total) were stored under “isothermal” conditions in a desiccator at 18 – 22 °C. Unlike other tin whisker studies, they were not exposed to thermal cycling or a corrosive (from solder flux) environment. The inspection stages were mainly limited to an examination of the compressive inside surfaces of the C-rings. Some observations were recorded relating to the outer tensile loaded surfaces and to the small, high-stress locations where the bolt/washer contacted the outer plated layer.

2.3 Examination of Whisker Growths

The C-ring surfaces were examined by visual means using a stereo-zoom binocular microscope and by scanning electron microscopy. Nine inspections stages have been performed since the specimen were plated, commencing at day 3 and finally at day 11,102. A total of 2160 data points have been tabulated. An evaluation of the structure and growth directions have been made using X-ray diffraction and transmission electron microscopy. Those findings and the results of an attempt to produce allotropic transformations in tin whiskers can be seen in the original 1987 report [1].

2.4 Microstructural Characterisation

Metallography was also conducted on one sample, covering each specimen variant. The sample was carefully cut from the C-ring with a jeweller’s saw. These pieces were mounted in a low exothermic resin and transversely sectioned to reveal the true plating thickness. The microsections were polished and examined by optical and electron microscopy. Scanning electron microscopy (SEM) was carried out using either a Carl Zeiss Leo 1530 VP FEG SEM equipped with an Oxford Instruments X-Max 80mm^2 detector for energy dispersive X-ray spectroscopy (EDS) or a Hitachi TM3030 benchtop scanning electron microscope.

3. Results

3.1 Characterisation of microsectioned 32 year old specimens

Detailed electron microscopy and elemental analysis has been undertaken to investigate the intermetallic growth present at the interface between the Sn coating and the brass and steel substrates, both with and without a copper barrier layer. These analyses have primarily focussed on the 'normal' tin deposits, including those fused after Sn deposition. The results of these analyses are presented in the following sections.

3.1.1 Sn deposits on brass with and without Cu barrier layers

The backscattered electron images in Figure 4 show the morphology and thickness of the intermetallic layer formed between 'normal' electroplated Sn coatings and brass substrates with and without Cu barrier layers. For tin deposited directly onto brass (Figure 4a), the Sn-Cu intermetallic layer is much less uniform than that formed with a copper barrier layer present (Figure 4b); this suggests that Cu diffusion is enhanced along the tin grain boundaries, which are also more readily identified for the sample deposited without the Cu barrier layer. It is also evident that the interface between the intermetallic layer and the brass substrate it less planar and also less distinct than that between the intermetallic and the Cu barrier layer. Each of these observations is likely to result from the Zn diffusion that occurs from the underlying brass substrate into the Sn deposit [9]. The x-ray maps shown in Figure 5 underline the irregular shape of the Cu-Sn intermetallic and confirm the presence of Zn along the Sn grain boundaries and, in particular, at the surface of the Sn deposit where it is present as Zn oxide. For the sample with the 3 µm Cu barrier layer the thickness of the intermetallic layer is more uniform with an average thickness of ~ 2.5 µm whilst the thickness of the remaining unreacted Cu layer is ~ 2.5 µm. In the presence of the Cu barrier layer, no measureable Zn diffusion into the Sn coating is evident; this is supported by SEM/EDX line scan analyses (Figure 6), which show that the extent of Zn diffusion into the Cu is limited and that little or no Zn is present beyond 1 µm into the Cu barrier layer. Only a single type of intermetallic phase is observed for both Sn deposits on brass and Sn deposits on brass with the Cu barrier layer; in both cases, the analysed composition of the intermetallic phase is consistent with Cu_6Sn_5.

For samples fused after Sn deposition (Figure 7), a distinct difference in intermetallic formation is observed for samples with and without the Cu barrier layer present. For the fused tin samples deposited directly onto brass two distinct layers are observed (Figure 7a). The first layer (Layer 1 in Figure 7a), adjacent to the brass substrate, has a uniform thickness of ~ 1.5 μm and is shown by EDX mapping (Figure 8) to contain Zn in addition to Cu and Sn. The approximate composition of this layer is 43% Cu, 21% Sn and 36% Zn (all at%). Beneath this layer, a region enriched in Cu and depleted in Zn is present within the brass. The intermetallic layer adjacent to the Sn coating (Layer 2 in Figure 7a) is thinner and generally less uniform with globular islands extending into the Sn deposit. EDX mapping (Figure 8) indicates that the Zn content within this layer is greatly reduced. Evidence of zinc oxide formation at the surface of fused tin deposits on brass has been observed by EDX mapping.

For the fused Sn deposit with the Cu barrier layer islands of globular intermetallic are present dispersed throughout the entire thickness of the Sn coating. In addition, an approximately uniform layer of intermetallic is present at the interface, which is comparable in thickness to that formed on the unfused sample (Figure 4b). EDX analysis shows that the composition of the intermetallic phase at the interface between the fused Sn and the Cu is consistent with that of Cu_6Sn_5. In comparison, the intermetallic phase present within the fused tin coating has a tin content that is ~10 at% higher than that of the interfacial intermetallic. SEM/EDX mapping (Figure 9) shows that with the Cu barrier layer present no Zn diffusion into the fused Sn deposit is observed and zinc oxide is not present at the deposit surface.

3.1.2 Sn deposits on steel with and without Cu barrier layers

Backscattered electron images showing the interface microstructure of 'normal' Sn deposits on steel, with and without Cu barrier layers, are shown in Figure 10. Higher resolution secondary electron images of the interface microstructure are shown in Figure 11. For Sn deposited directly onto the steel substrate (Figures 10a and 11a) there is no clear evidence of intermetallic formation after 32 years storage at room temperature. For the sample with

the Cu barrier layer (Figures 10b and 11b), the Sn-Cu intermetallic, shown by EDX analysis to be Cu_6Sn_5 with an average composition of 53.4 ± 1.3 at% Cu and 46.6 ± 1.3 at% Sn, is relatively planer and similar in both thickness and morphology to that formed for the Sn deposits on brass with the Cu barrier layer. The average thickness of the intermetallic layer is ~ 2.2 ± 0.5 µm whilst the thickness of the unconsumed Cu barrier layer is ~ 2.5 µm, i.e. comparable to that observed for the Sn deposits on brass with the Cu barrier layer. The EDX maps shown in Figure 12 indicate that little, if any, interdiffusion has occurred between the Cu barrier layer and the steel substrate. In the case of the fused Sn deposit on steel, fine Fe-Sn intermetallic particles are present at the interface (Figure 11c). The precise composition of these features is not known since their fine scale precludes accurate compositional analysis by SEM+EDX techniques. For the fused Sn deposit on steel with the Cu barrier layer present (Figure 10d), intermetallic formation is similar to that observed for the Sn deposit on brass with the Cu barrier layer, i.e. large discrete globular intermetallic particles are present within the Sn coating in addition to the relatively planer layer of intermetallic at the interface. Typically, the intermetallic present within the Sn coating has a slightly higher Sn content than the intermetallic present at the interface (~ 51 at% Sn compared with ~ 47 at% Sn). It is interesting to note that the potential for continued whisker growth remains even after 32 years storage. This is demonstrated by the growth of new whiskers on freshly prepared cross sections, an example of which is shown in Figure 13 for a Sn deposit on steel with a Cu barrier layer.

3.2 Evaluation of whisker growth

Tin whiskers have been seen to nucleate and grow from all of the as-plated C-ring surfaces. The nucleation period prior to growth was short for those tin platings that had been applied either directly onto a brass substrate or to a copper intermediate layer. The “normal” commercial tin plating was observed to support the largest initial rates of growth, followed by the “abnormal” high current density tin-plating. The lengths of these whiskers were in excess of 0.5mm after a shelf life of only 2 months. The tin-plated steel with a copper barrier, like those of brass with a copper barrier, grew to lengths in the order of 4.5mm

when examined at the 32-year inspection. Whiskers grown on both tin plated brass and tin plated steel with a Cu barrier layer possessed a wide range of growth morphologies including straight filaments, kinked filaments, multidirectional whiskers and odd shaped eruptions. Examples of the various growth morphologies, observed during the last inspection, are shown in Figures 14 and 15 for tin plated steel with a copper barrier layer and tin plated brass, respectively. The organically contaminated platings were slow to nucleate whiskers and needed between 6 months and 3 years before any whiskers nucleated, they then grew during the next 12 years to lengths of between 1 and 2.2mm. The "normal" tin plating made directly to the mild steel substrates incurred extremely long nucleation periods of approximately 6 months. No whiskers were seen to nucleate on any of the fused tin-plated layers.

An attempt was made to calculate the whisker density on the samples, but this was abandoned because of the random nature of growths and the fact that this task would be exceedingly time-consuming. Several estimates were made, they ranged from 0.1 to 200/mm^2. For completeness, all of the inspection results have been compiled into Tables 2-6.

4. Discussion

The measured length of the longest whisker as a function of storage time is plotted in Figure 16 for the "normal" tin deposits on brass and steel with and without a copper barrier layer present. Results show that with an barrier layer present, whisker growth for tin deposits on brass and steel was comparable, i.e. the rate and extent of whisker growth was independent of the substrate material and solely determined by the growth of the Cu_6Sn_5 intermetallic at the Cu-Sn interface due to the limited diffusion of both Zn and Fe into the Cu barrier layer and their absence within the tin coating. Figure 16 also shows that the onset of whisker growth occurred more quickly, and the maximum whisker length was greater, for tin deposits on brass compared with the other samples. This observation is consistent with other studies that have demonstrated increased whisker growth for tin deposits on brass

compared with tin deposits on copper [9]–[11]. Increased whisker growth for tin deposits on brass can be attributed to Zn diffusion into the tin from the underlying substrate with the subsequent formation of zinc oxide at the deposit surface [9]. Although it is generally accepted that Sn deposits on brass are more susceptible to whisker growth than those on Cu, there have been reports of reduced whisker growth for tin deposits on brass compared with Cu [12][13]. In each of these papers the authors attributed a decrease in whisker growth to a reduction in the rate at which the Cu_6Sn_5 intermetallic was formed, i.e. the presence of Zn suppressed the growth of the Cu_6Sn_5 thereby reducing the driving force for whisker growth. In the present study, although there is a clear difference in the morphology of the intermetallic formed between tin deposits on brass and those on Cu (Figure 4) the amount of intermetallic formed is comparable. It should be noted that neither of the aforementioned papers considered the impact of Zn diffusion into the tin deposit on whisker growth. With the 3 µm Cu barrier layer present, Zn diffusion into the Sn deposit is limited, even over a 32 year timescale (Figure 6), and the additional driving force for whisker growth is removed. For tin deposits on steel without a barrier layer no intermetallic formation is observed, even after 32 years ambient storage, and no whisker growth is observed. For fused tin deposits on steel, although fine (<1 µm), discrete intermetallic particles are present at the interface, no whisker growth is observed. In the case of fused tin deposits on brass, no whisker growth was observed, irrespective of whether a copper barrier layer was present or not.

For tin deposits onto brass and steel with the Cu barrier layer present the thickness of the intermetallic layer after 32 years storage was ~ 2.5 µm in both cases. This suggests that the Cu_6Sn_5 functions as an effective diffusion barrier to the continued formation of intermetallic compound such that a significant proportion of the Cu barrier layer remains unreacted even after 32 years storage at room temperature. It is also interesting to note that the intermetallic layer is relatively planar and does not possess an overtly pronounced ‘wedge-shaped’ morphology that is often associated with an increased propensity for whisker growth [14][15].

5. Conclusions

1. For normal tin electroplated onto brass, a one or two month nucleation period was needed before whiskers were seen to develop. They reached a maximum length of about 1.5 mm after 6 months. Little or no growth occurred during the intervening 30 years. However, deposits from contaminated tin baths needed up to 3 years before nucleation, and these whiskers subsequently grew to lengths of up to 2.2 mm.
2. Extensive zinc oxide formation was observed at the surface of normal tin deposits after storage for 32 years. The introduction of a Cu barrier layer reduced the rate of whisker growth by inhibiting zinc diffusion into the Sn deposit and thereby preventing the formation of zinc oxide on the surface of the deposit.
3. Normal tin plated samples with a copper barrier layer nucleated whiskers within 5 months and these grew to lengths between 1 and 4.5 mm. For tin deposits on brass and steel with a copper barrier layer whisker growth was comparable; due to the fact that comparable intermetallic compound formation occurred in both cases and elemental diffusion from the substrate into the Sn deposit was supressed.
4. Contaminated tin on copper gave an unexpected result: one sample only nucleated whiskers during the final 12 years storage and they grew to 1.8 mm.
5. After 32 years storage, the Cu_6Sn_5 intermetallic layer was ~ 2.5 µm thick for both Sn deposits on brass and Sn deposits on steel with a copper barrier layer. In both cases a significant fraction of the original Cu plating remained unreacted.
6. None of the fused tin-platings nucleated or grew whiskers during the 32 years storage period (i.e. fused tin on brass, copper-plated brass and steel). The absence of whisker growth for these samples results from the formation of a more uniform intermetallic compound at the interface and the removal of the as-deposited tin microstructure. For the fused tin deposits on brass the formation of the intermetallic layer during the fusing process most likely serves to inhibit subsequent Zn diffusion through the Sn deposit, thereby mitigating whisker growth. In the case of fused tin deposits on steel only fine scale (~1µm) discrete intermetallic growth is observed.

7. No whisker growth was observed for tin deposits on steel and after 32 years no intermetallic formation was observed.

8. Whiskers are seen to possess numerous morphologies, including straight and multidirectional filaments, and typically have diameters ranging from 1 to 20µm. Their density appears to vary from about 0.1 to 200/mm^2.

6. References

[1] B. D. Dunn, “A laboratory study of tin whisker growth,” *Eur. Sp. Agency Rep. STR-223, Eur. Sp. Agency, Paris, Fr.*, 1987.

[2] B. D. Dunn, “15½ years of tin whisker growth, ESTEC Materials Report 4562,” Noordwijk, the Netherlands, 2006.

[3] B. D. Dunn, “Whisker formation on electronic materials,” *Circuit World*, vol. 2, no. 4, pp. 32–40, 1976.

[4] B. D. Dunn, “Mechanical and electrical characteristics of tin whiskers with special reference to spacecraft systems,” *ESA J.*, vol. 12, pp. 1–17, 1988.

[5] B. D. Dunn, “An overview of whisker problems on ESA space hardware,” in *3rd International Symposium on Tin Whiskers (2009)*.

[6] “ECSS-Q-ST-70-08C (2009) The manual soldering of high reliability spacecraft assemblies, ESA Publications Division, Noordwijk, The Netherlands, August 1999.”

[7] The European Parliament and The Council of The European Union, “Directive 2002/95/EC of the European Parliament and the Council of 27 January 2003 on the restriction of the use of certain hazardous substances in electrical and electronic equipment,” *Off. J. Eur. Union*, vol. 46, no. February, p. L37 19–23, 2003.

[8] ASTM, *Standard practice for making and using C-ring stress-corrosion test specimens, ASTM G38-01*. 2013.

[9] M. A. Ashworth, G. D. Wilcox, R. L. Higginson, R. J. Heath, and C. Liu, “An investigation into zinc diffusion and tin whisker growth for electroplated tin deposits on brass,” *J. Electron. Mater.*, vol. 43, no. 4, pp. 1005–1016, 2014.

[10] S. C. Britton and M. Clarke, “Effects of Diffusion from Brass Substrates Into Electrodeposited Tin Coating on Corrosion Resistance and Whisker Growth,” *Trans. Inst. Met. Finish.*, vol. 40, pp. 205–211, 1964.

[11] M. A. Ashworth, G. D. Wilcox, R. L. Higginson, R. J. Heath, C. Liu, and R. J. Mortimer, “The effect of electroplating parameters and substrate material on tin whisker formation,” *Microelectron. Reliab.*, vol. 55, no. 1, pp. 180–191, 2015.

[12] S. M. Miller, U. Sahaym, and M. G. Norton, “Effect of Substrate Composition on Sn Whisker Growth in Pure Sn Films,” *Metall. Mater. Trans. a-Physical Metall. Mater. Sci.*, vol. 41A, no. 13, pp. 3386–3395, Dec. 2010.

[13] J. Stein, C. A. Cordova Tineo, U. Welzel, W. Huegel, and E. J. Mittemeijer, “Microstructural Development and Possible Whiskering Behavior of Thin Sn Films Electrodeposited on Cu(Zn) Substrates,” *J. Electron. Mater.*, vol. 44, no. 3, pp. 886–894, 2014.

[14] A. Baated, K.-S. Kim, and K. Suganuma, “Effect of intermetallic growth rate on spontaneous whisker growth from a tin coating on copper,” *J. Mater. Sci. Mater. Electron.*, vol. 22, no. 11, pp. 1685–1693, Mar. 2011.

[15] K. S. Kim, C. H. Yu, S. W. Han, K. C. Yang, and J. H. Kim, “Investigation of relation between intermetallic and tin whisker growths under ambient condition,” *Microelectron. Reliab.*, vol. 48, no. 1, pp. 111–118, Jan. 2008.

Figures

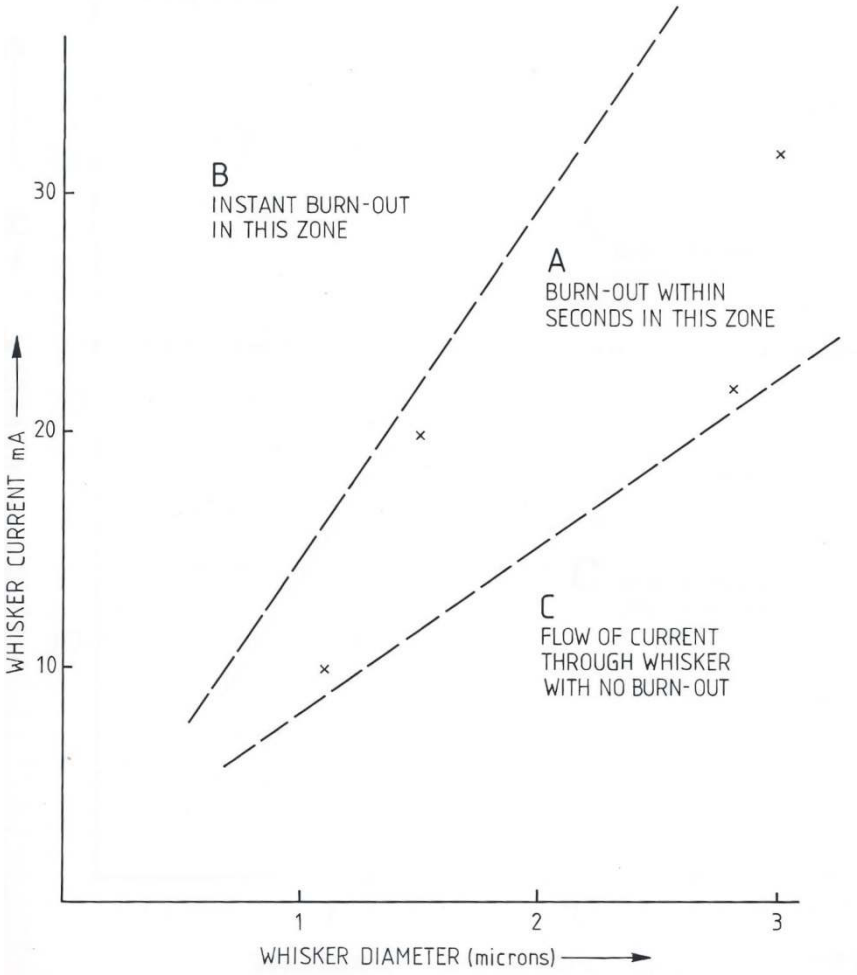

Fig. 1 Graph to illustrate the effect of whisker diameter on possible short circuiting whisker (from plots of mA vs mV for four whiskers, relationship is linear until heating effects cause whisker burn out). These measurements were made on actual whiskers. Whisker currents depicted in 'region C' could account for the intermittent short-circuits encountered on spacecraft equipment.

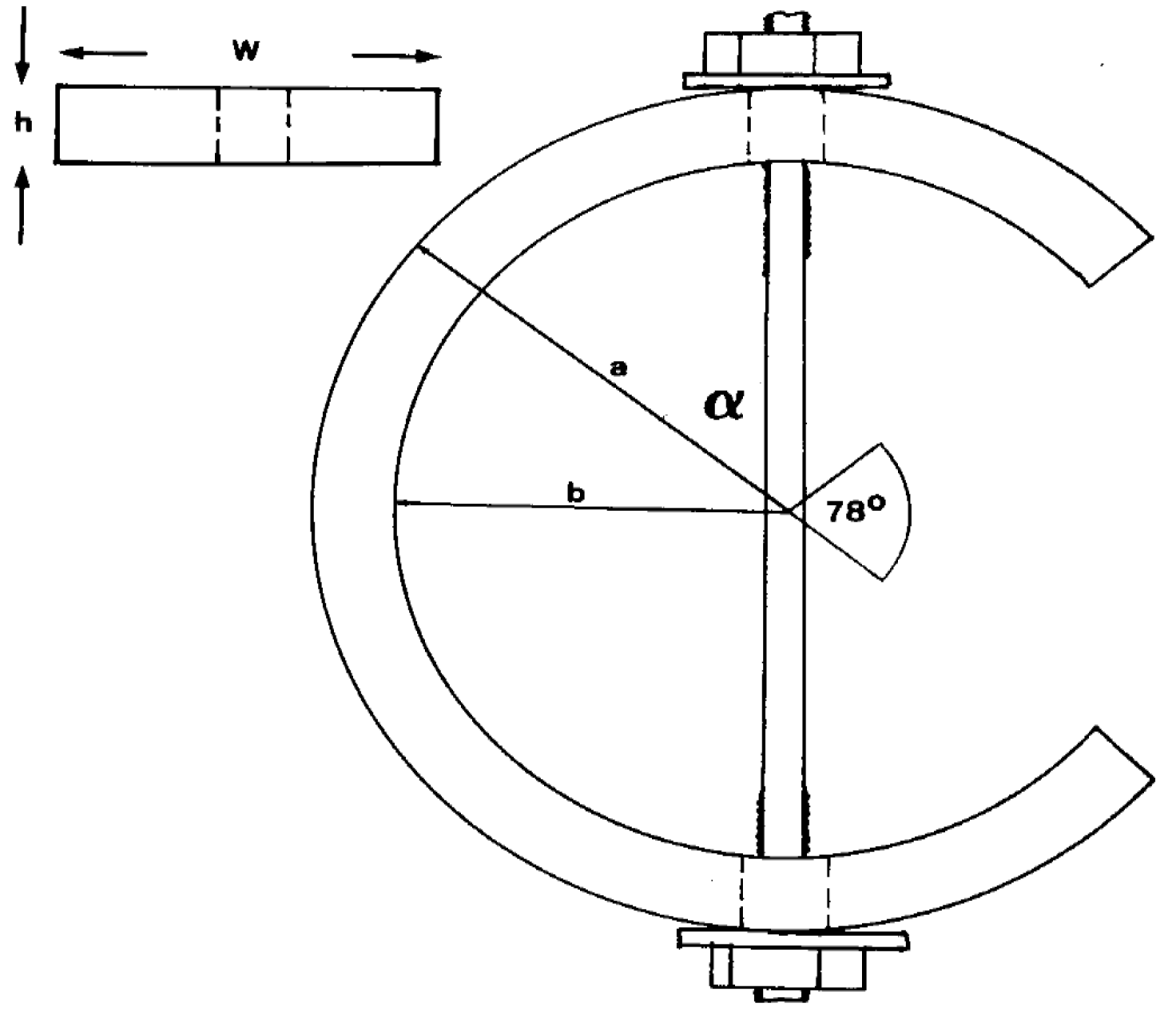

Figure 2 Overall dimensions for C-ring specimens. W = width = 25mm, h = thickness = 2mm, a = outside radius = 12.5mm, b = inside radius = 10.5mm

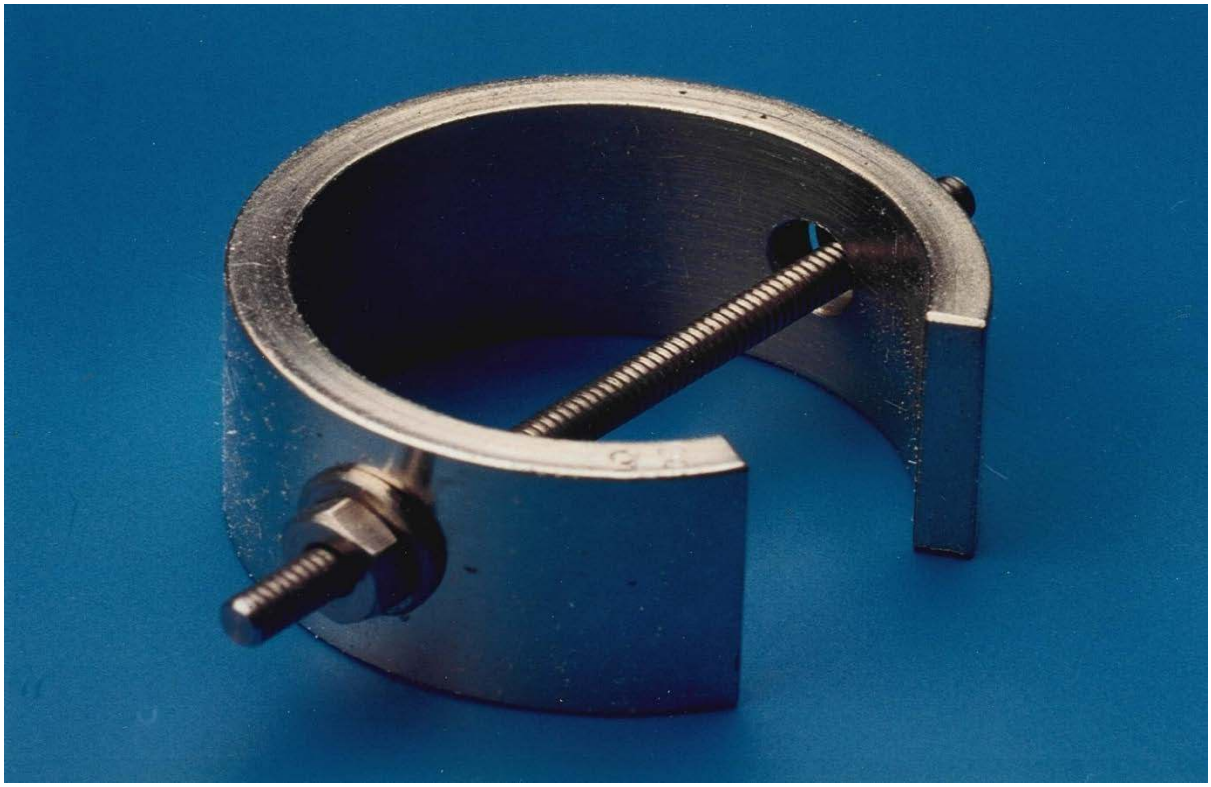

Figure 3 Optical photograph of typical C-ring. Some long whisker growths can be discerned on both the inner and outer surfaces.

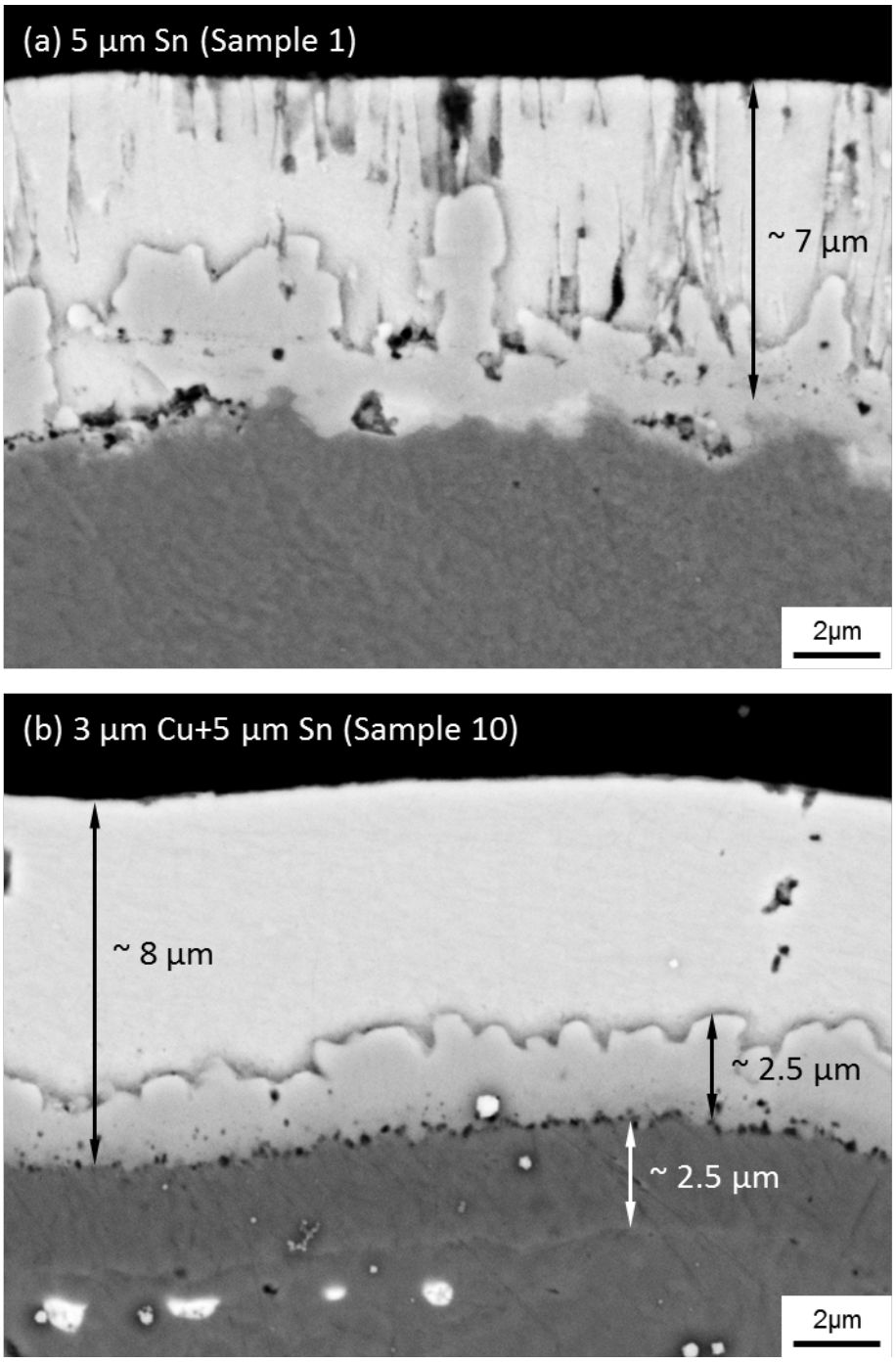

Figure 4 Backscattered electron images showing the interfacial regions of normal Sn deposits on brass after storage at room temperature for 32 years: (a) 5 µm Sn deposit, (b) 5 µm Sn deposit with a 3µ m Cu barrier layer

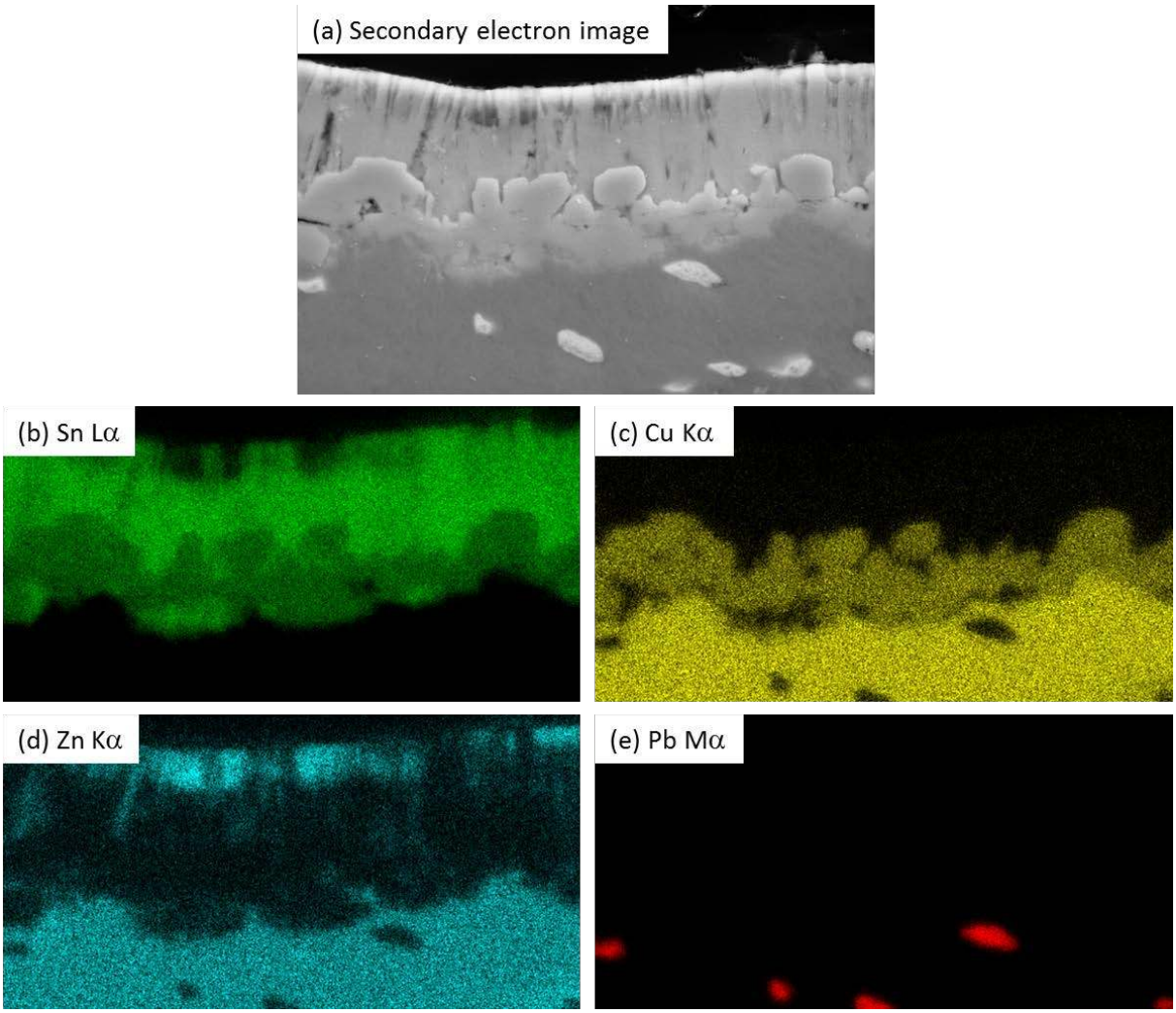

Figure 5 SEM/EDX analysis of a cross-sectioned Sn deposit on brass after storage at room temperature for 32 years: (a) secondary electron image, (b) Sn L α x-ray map, (c) Cu K α x-ray map, (d) Zn K α x-ray map and (e) Pb M α x-ray map

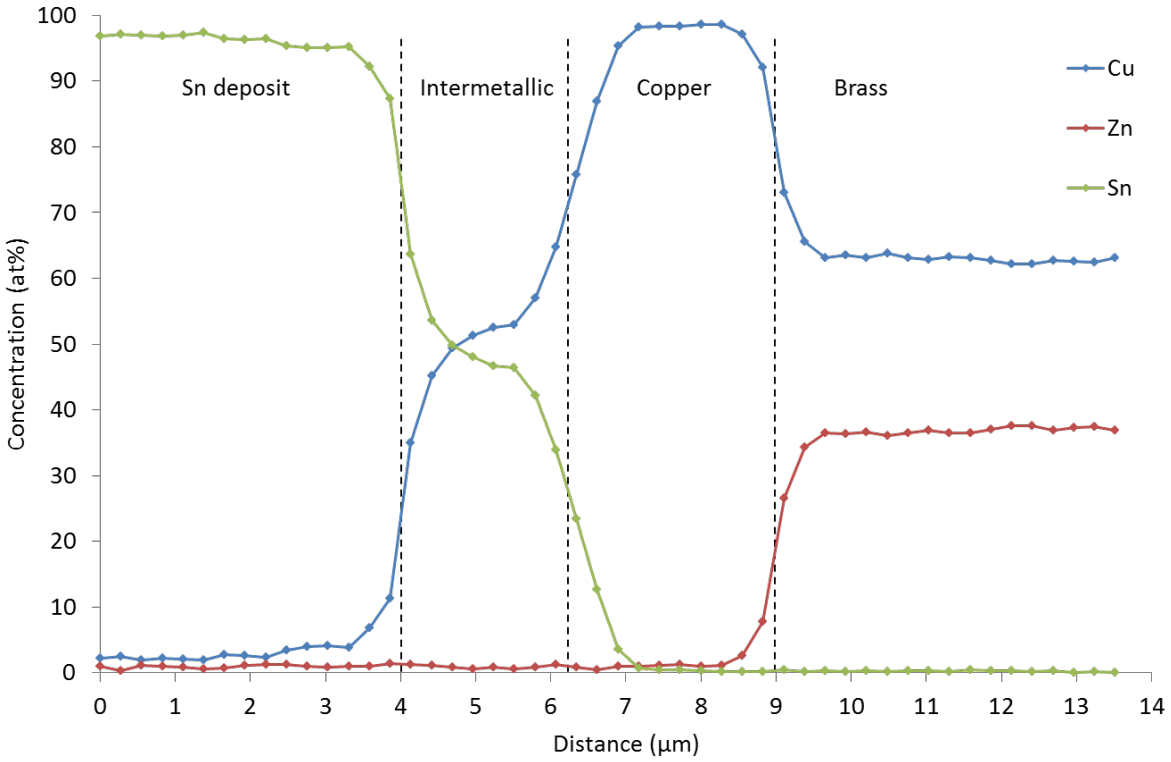

Figure 6 SEM/EDX line scan showing the elemental distribution across the interfacial regions of a 5 µm Sn deposit on brass having a 3 µm Cu barrier layer after storage at room temperature for 32 years

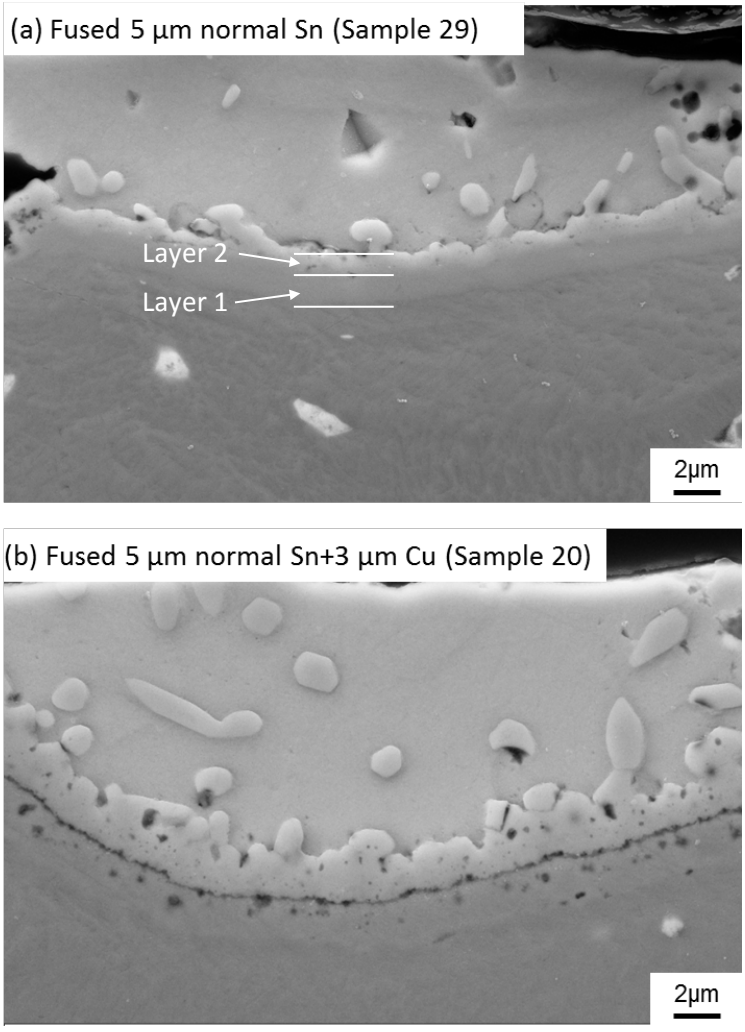

Figure 7 Secondary electron images showing the extent of intermetallic formation for fused 'normal' Sn deposits on brass after storage at room temperature for 32 years: (a) 5 µm fused Sn deposit and (b) 5 µm fused Sn deposit with a 3 µm Cu barrier layer.

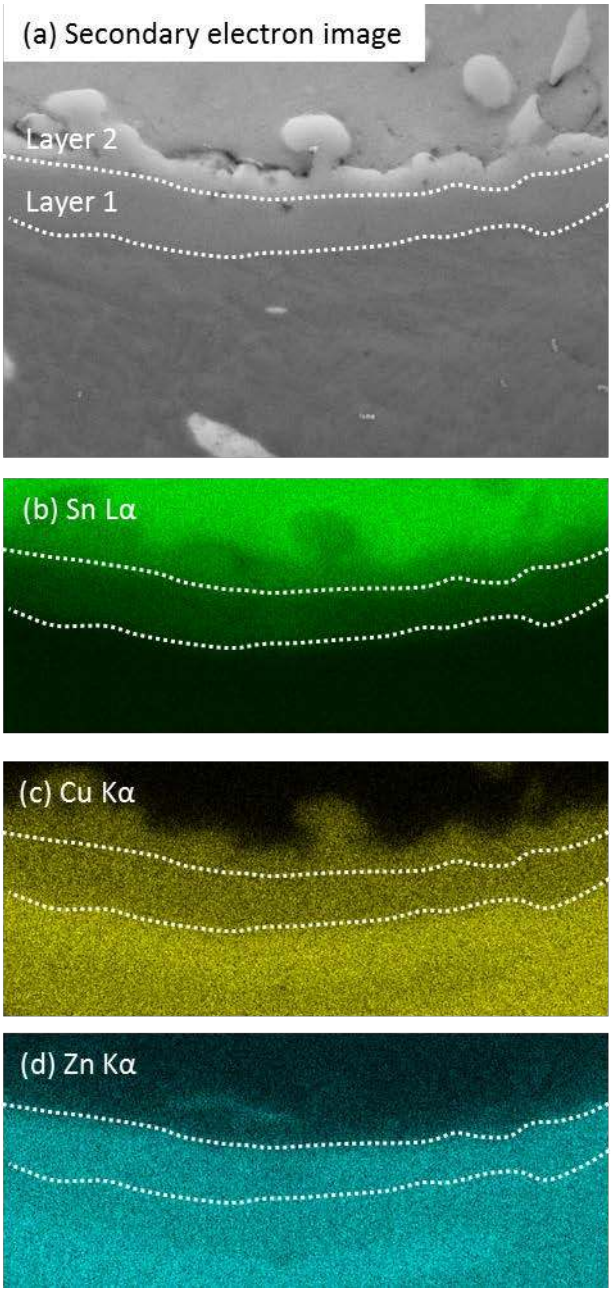

Figure 8 SEM/EDX analysis of a cross-sectioned fused Sn deposit on brass after storage at room temperature for 32 years: (a) secondary electron image, (b) Sn L α x-ray map, (c) Cu K α x-ray map, (d) Zn K α x-ray map

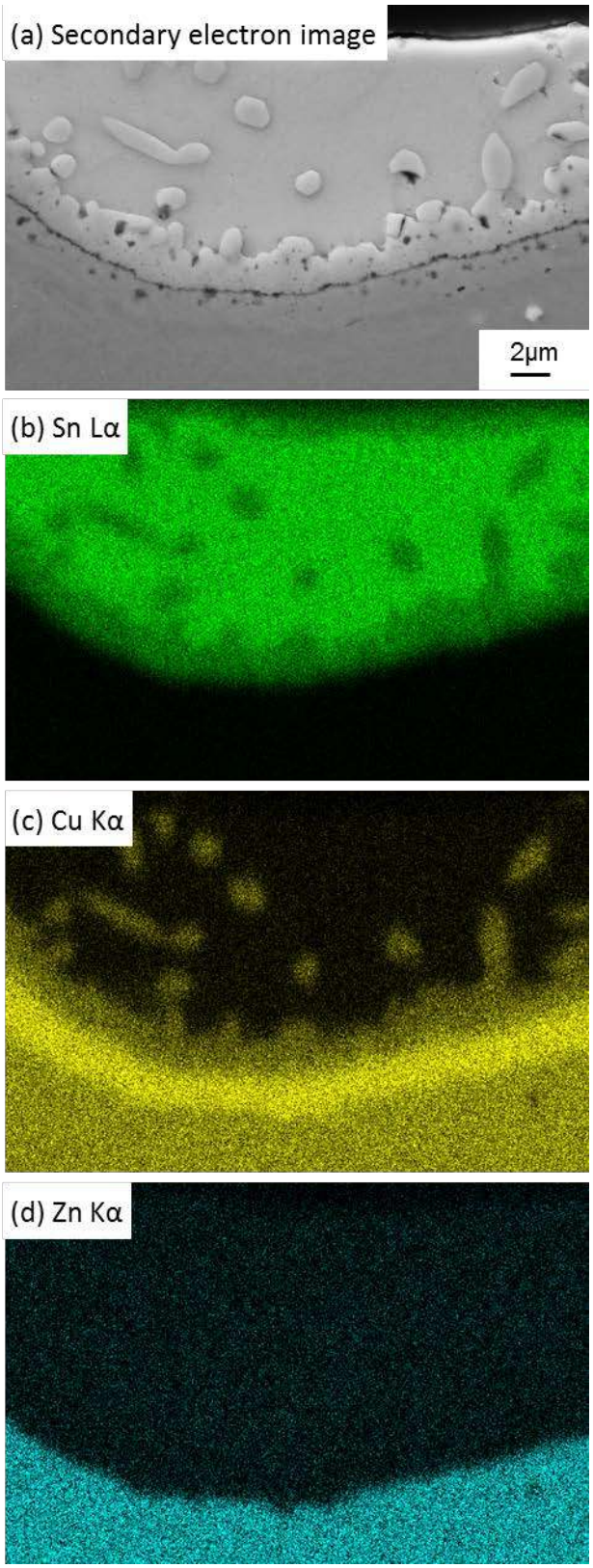

Figure 9 SEM/EDX analysis of a cross-sectioned fused Sn deposit on brass with a 3 µm Cu barrier layer after storage at room temperature for 32 years: (a) secondary electron image, (b) Sn L α x-ray map, (c) Cu K α x-ray map, (d) Zn K α x-ray map

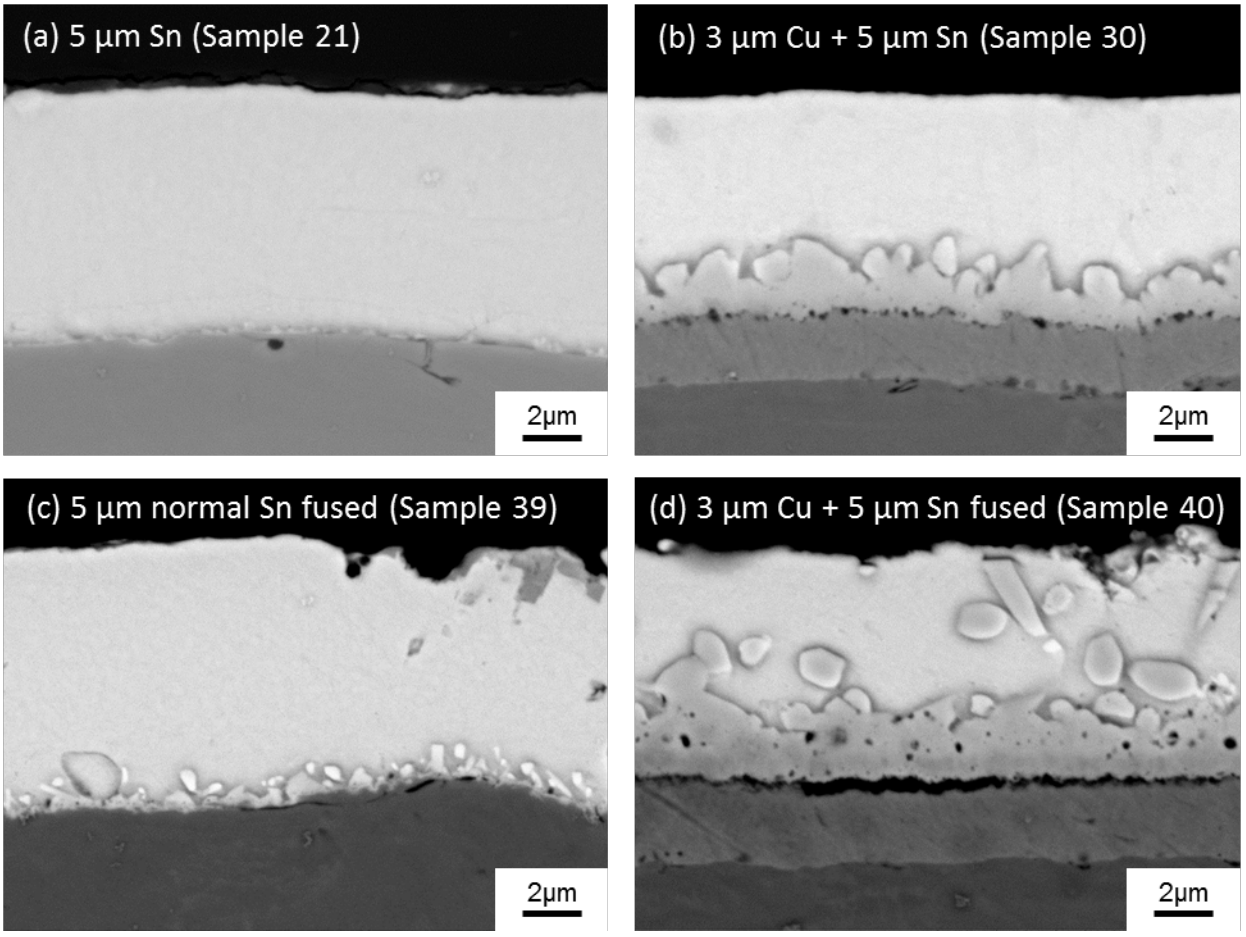

Figure 10 Back-scattered electron images showing the extent of intermetallic formation for normal Sn deposits on steel after storage at room temperature for 32 years: (a) 5 µm Sn deposit, (b) 5 µm Sn deposit with a 3 µm Cu barrier layer, (c) a fused 5µm Sn deposit and (d) a fused 5µm Sn deposit with a 3 µm Cu barrier layer

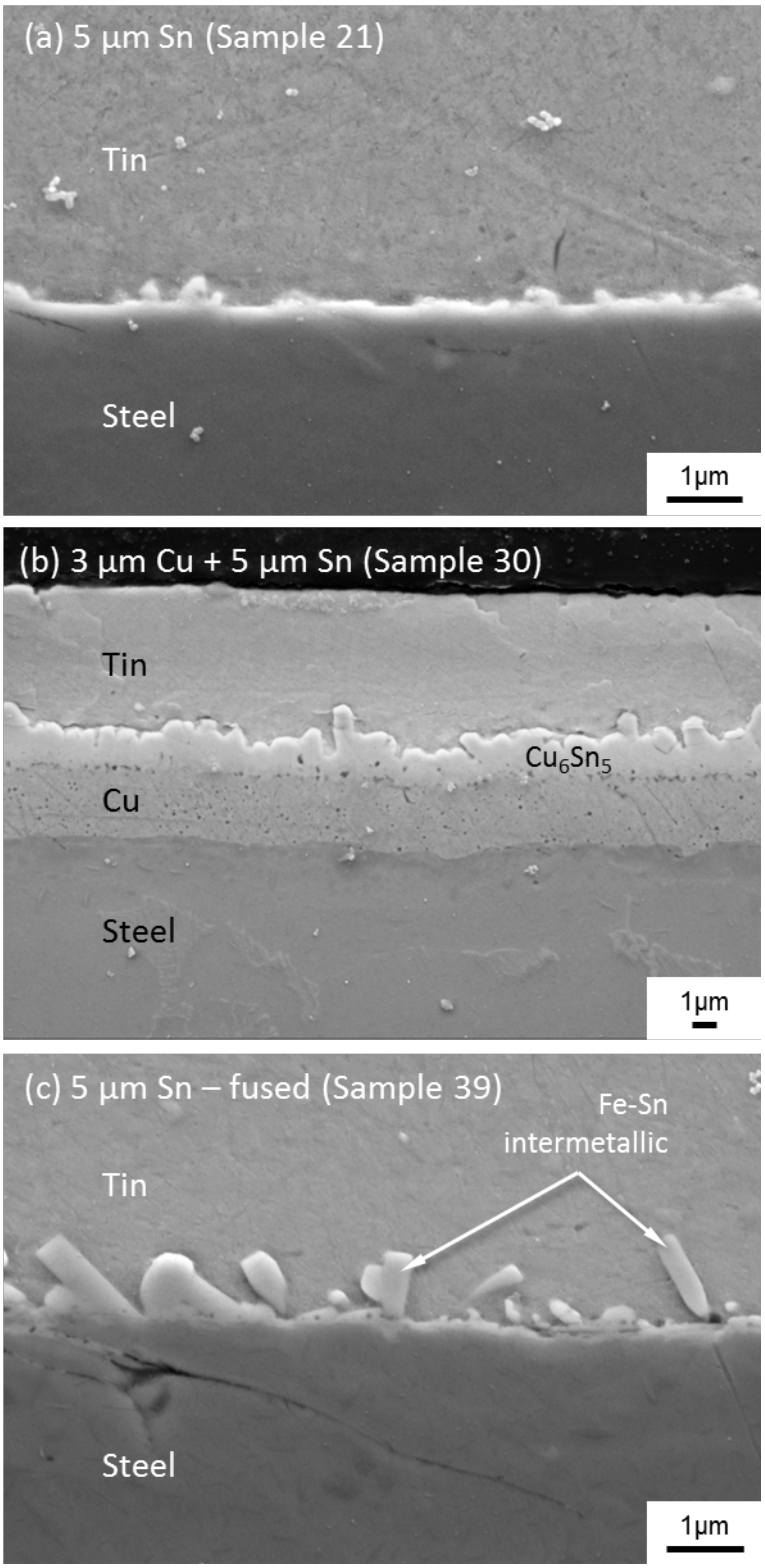

Figure 11 High magnification secondary electron images showing the interface regions of normal Sn deposits on steel after storage at room temperature for 32 years: (a) 5 µm Sn deposit, (b) 5 µm Sn deposit with a 3 µm Cu barrier layer and (c) a fused 5µm Sn deposit

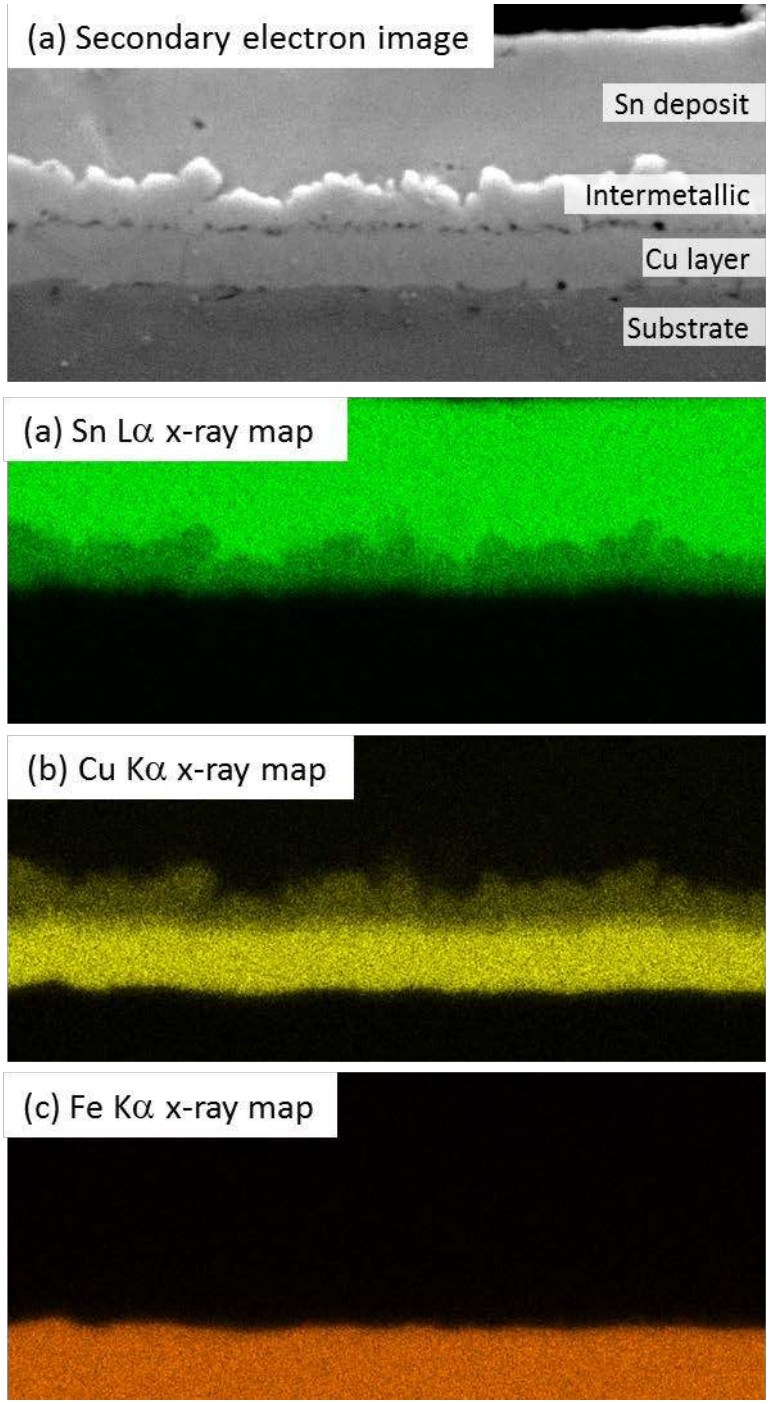

Figure 12 SEM/EDX analysis of a cross-sectioned Sn deposit on steel with a 3µm barrier layer after storage at room temperature for 32 years: (a) secondary electron image, (b) Sn L α x-ray map, (c) Cu K α x-ray map, (d) Fe K α x-ray map

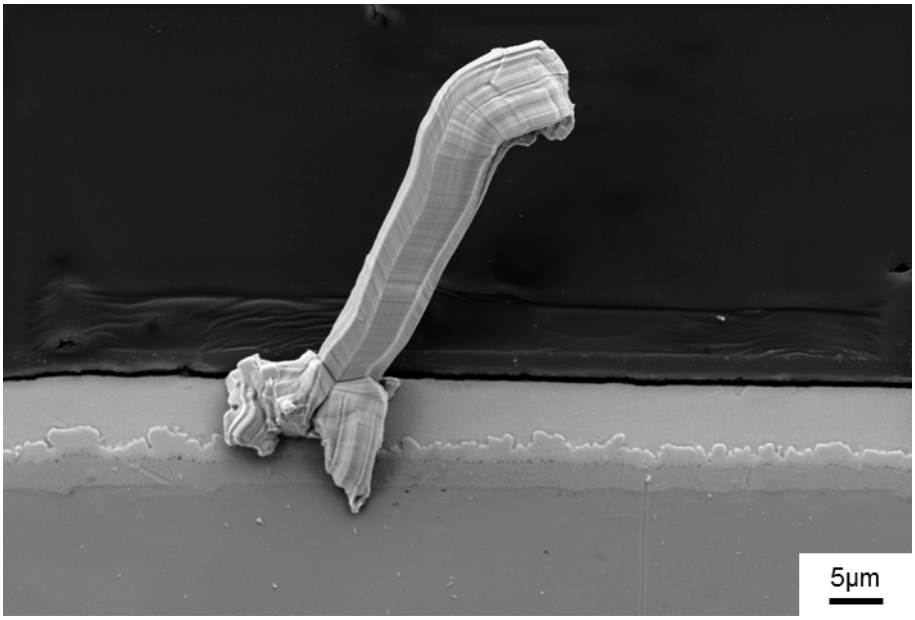

Figure 13 Secondary electron image showing whisker growth from the polished surface of a cross-sectioned Sn deposit on steel with a 3 µm Cu barrier layer.

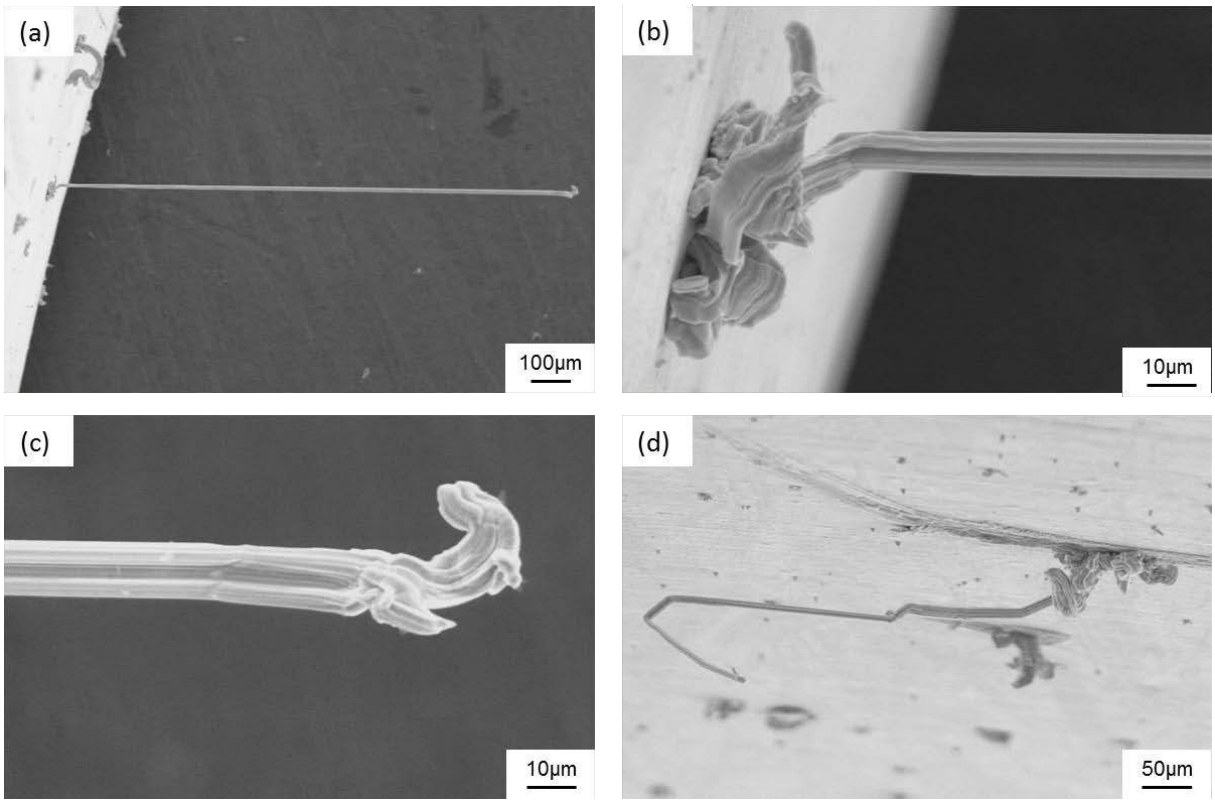

Figure 14 Scanning electron microscope images from the last inspection of a normal Sn deposit on steel with a 3 µm Cu barrier layer (sample 30), showing (a) a typical straight filament whisker having, (b) a kinked portion at its base, (c) an irregular tip and (d) multidirectional growth

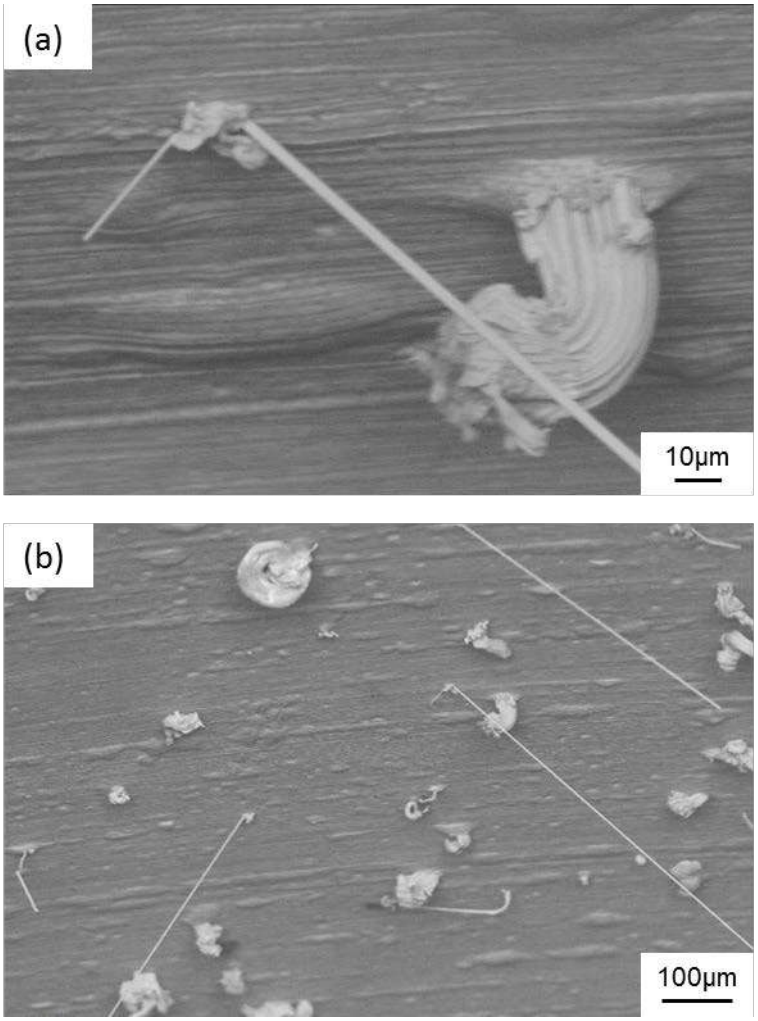

Figure 15 Scanning electron microscope images from the last inspection of a Sn deposit on brass (sample 8), showing (a) three whiskers of varying diameters, from 1µm (short length), 2 µm long length and 20 µm appearing as a stubby eruption and (b) a whisker density of about 90/mm2

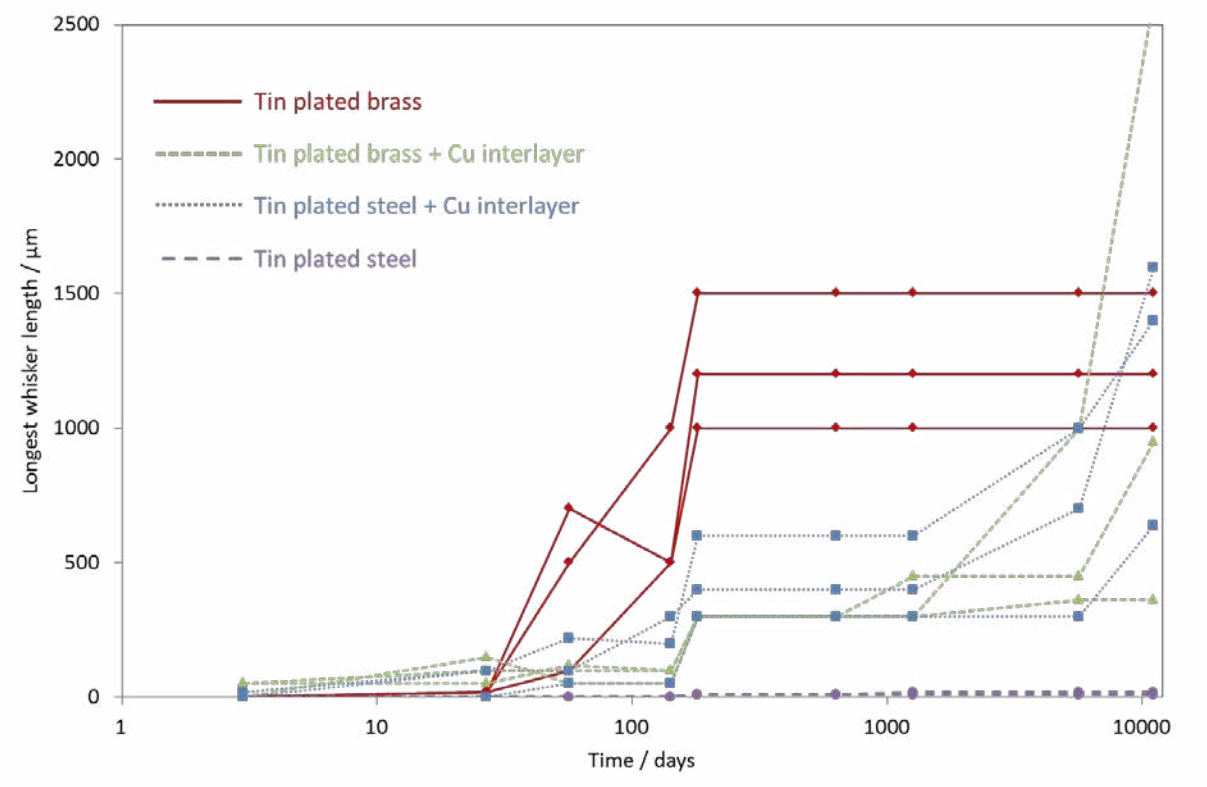

Figure 16 Graph comparing the length of the longest whisker as a function of storage time at room temperature for unstressed normal tin deposits on brass and on steel with and without a copper barrier layer present

Tables

Table 1 Bath conditions for the various platings (Note. All chemical analyses were confirmed by analysis reports from the Oxymetals Benelux Laboratory).

	Normal tin	Abnormal tin	Organically contaminated tin
Tin as stannous sulphate (g/l)	40	7.5	40
Free sulphuric acid (g/l)	160	160	160
Oxymetal brightener no. 4 (cc/l)	10	10	10
no.5 (cc/l)	4	4	4
no.6 (cc/l)	20	20	20
Organic flour contamination	none	none	Handful
Bath temperature	20°C	50°C	30°C
Current density (agitated bath)	1.5 A/dm^2	5 A/dm^2	1.5 A/dm^2

Table 2 Growth on tin-plated brass substrate

SPECIMEN NO.	TYPE OF TIN	STRESS LEVEL		INSPECTION PERIOD (d) LENGTH OF WHISKERS (μm)								
				(V)3	(S)27	(S)57	(V)142	(S)181	(S)634	(S)1269	(S)5657	(S)11102
1	NORMAL	NONE	A	0	20	100	500	1000	1000	1000	1000*	1000*
			B	0	20	700	500	1200	1200	1200	1200	1200
			C	0	20	500	1000	1500	1500	1500	1500	1500
2		SLIGHT	A	20	0	50	100	1000	1000	1000	1000*	1000*
			B	0	0	0	300	1000	1000	1000	1000	1000
			C	0	0	70	300	1500	1500	1500	1500	1500
3		HIGH	A	0	0	50	100	200	200	200	200	525
			B	0	0	20	100	200	600	600	600	600
			C	0	0	100	100	150	250	250	250	250
4	ABNORMAL	NONE	A	0	0	35	0	50	50	50	50	50
			B	0	50	120	100	150	150	150	150	150
			C	0	0	0	0	10	10	10	10	10
5		SLIGHT	A	0	0	35	30	50	50	50	50	50
			B	20	20	100	100	100	100	100	100	100
			C	0	0	10	0	50	50	50	50	50
6		HIGH	A	0	0	60	0	200	200	200	200	200
			B	0	0	50	100	600	600	600	600	600
			C	0	0	10	0	10	10	10	30	30
7	CONTAMINATED	NONE	A	0	0	0	0	60	80	80	900	900
			B	0	0	0	0	0	0	1600	2000	2000
			C	0	0	0	0	50	50	200	200	200
8		SLIGHT	A	0	0	0	0	180	180	1200	2000	2000
			B	0	0	0	0	100	100	400	2200	2400
			C	0	0	0	0	0	0	400	1000	1000
9		HIGH	A	0	0	0	0	1000	1000	1000	1500	1500
			B	0	0	10	0	200	200	200	200	200
			C	0	0	0	0	100	100	100	100	100

Table 3 Growths on tin-plated brass with copper barrier

SPECIMEN NO.	TYPE OF TIN	STRESS LEVEL (Table 3)		INSPECTION PERIOD (d) LENGTH OF WHISKERS (μm)								
				(V)3	(S)27	(S)57	(V)142	(S)181	(S)634	(S)1269	(S)5657	(S)11102
10	NORMAL	NONE	A	50	50	120	100	300	300	300	360	360
			B	0	150	50	50	300	300	450	450	950
			C	50	100	100	100	300	300	300	1000	2600
11		SLIGHT	A	50	200	500	500	500	500	500	700	1600
			B	50	100	140	200	600	600	600	1000	1000
			C	50	50	60	100	100	100	100	500	500
12		HIGH	A	0	20	20	0	50	50	450	500	580
			B	0	0	10	0	50	50	50	1000	1200
			C	0	0	0	0	50	50	50	500	500
13	ABNORMAL	NONE	A	0	0	100	100	150	200	200	3500*	3500*
			B	0	0	350	100	700	700	700	1000	1000
			C	0	0	10	0	10	10	10	950	950
14		SLIGHT	A	0	0	260	200	280	280	280	1000	1000
			B	0	0	300	300	300	300	300	2500	2500
			C	0	0	10	0	10	10	10	500	500
15		HIGH	A	50	300	600	600	1100	1100	1100	2000	3900*
			B	0	100	400	400	450	450	450	2500	2500
			C	0	100	300	300	600	600	600	600	600
16	CONTAMINATED	NONE	A	0	0	0	0	40	60	100	750	750
			B	0	0	0	0	40	40	50	250	940
			C	0	0	0	0	40	40	50	50	50
17		SLIGHT	A	0	0	0	0	200	200	200	1000	1200
			B	0	0	0	0	40	40	140	1500	1500
			C	0	0	0	0	40	40	40	500	1200
18		HIGH	A	0	0	0	0	20	20	20	20	250
			B	0	0	10	0	100	100	140	800*	1200*
			C	0	0	0	0	40	40	40	150	200

Table 4 Growths on tin plated steel substrate

SPECIMEN NO.	TYPE OF TIN	STRESS LEVEL (Table 3)		INSPECTION PERIOD (d) LENGTH OF WHISKERS (μm)								
				(V)3	(S)27	(S)57	(V)142	(S)181	(S)634	(S)1269	(S)5657	(S)11102
21	NORMAL	NONE	A	0	0	0	0	10	10	10	10	10
			B	0	0	0	0	10	10	20	20	20
			C	0	0	0	0	10	10	10	10	10
22		SLIGHT	A	0	0	0	0	10	10	10	10	15
			B	0	0	0	0	10	10	10	10	10
			C	0	0	0	0	10	10	10	10	10
23		HIGH	A	0	0	0	0	0	0	10	10	0
			B	0	0	0	0	0	0	15	15	0
			C	0	0	0	0	0	0	0	0	0
24	ABNORMAL	NONE	A	0	0	0	0	0	0	0	0	0
			B	0	0	0	0	0	0	0	0	0
			C	0	0	0	0	0	0	0	0	0
25		SLIGHT	A	0	0	0	0	0	0	0	0	0
			B	0	0	0	0	0	0	0	0	0
			C	0	0	0	0	0	0	0	0	0
26		HIGH	A	0	0	0	0	0	0	0	0	0
			B	0	0	0	0	0	0	0	0	0
			C	0	0	0	0	0	0	0	0	0
27	CONTAMINATED	NONE	A	0	0	0	0	0	0	0	0*	0
			B	0	0	0	0	0	0	0	0*	0
			C	0	0	0	0	0	0	0	0*	0
28		SLIGHT	A	0	0	0	0	0	0	0	0*	0
			B	0	0	0	0	0	0	0	0*	0
			C	0	0	0	0	0	0	0	0*	0
29		HIGH	A	0	0	0	0	0	0	0	0*	0
			B	0	0	0	0	0	0	0	0*	0
			C	0	0	0	0	0	0	0	0*	0

Table 5 Growths on tin plated steel with copper barrier

SPECIMEN NO.	TYPE OF TIN	STRESS LEVEL (Table 3)		INSPECTION PERIOD (d) LENGTH OF WHISKERS (μm)								
				(V)3	(S)27	(S)57	(V)142	(S)181	(S)634	(S)1269	(S)5657	(S)11102
30	NORMAL	NONE	A	0	100	220	200	600	600	600	1000	1400
			B	20	100	100	300	400	400	400	700	1600
			C	0	0	50	50	300	300	300	300	640
31		SLIGHT	A	0	50	200	200	250	250	250	1200*	1200*
			B	0	1000	225	200	300	300	300	500	700
			C	0	20	100	100	100	100	100	500	500
32		HIGH	A	0	200	400	400	500	500	500	1200	1950
			B	0	100	300	300	400	400	400	1000	1000
			C	0	100	500	500	500	500	500	1000	1000
33	ABNORMAL	NONE	A	0	100	20	100	600	600	600	4600*	4600*
			B	0	300	20	0	220	220	220	2000	2000
			C	0	0	20	0	100	100	100	2000	2000
34		SLIGHT	A	0	500	800	800	800	800	800	3500	3500
			B	0	0	50	50	50	50	50	2000	2000
			C	0	50	50	50	50	50	50	2000	2000
35		HIGH	A	20	500	1100	1200	1200	1200	1200	3000	3000
			B	0	100	425	500	600	600	600	1000	1000
			C	0	100	400	400	300	300	300	2500	2500
36	CONTAMINATED	NONE	A	0	0	0	0	0	50	100	1000	1000
			B	0	20	40	40	40	70	400	2000	2000
			C	0	0	0	0	0	0	350	1500	1500
37		SLIGHT	A	0	0	50	50	70	70	70	1500	1500
			B	0	20	50	50	70	70	400	2000	2000
			C	0	0	0	0	70	70	400	1000	1000
38		HIGH	A	0	0	0	0	0	0	0	1800	1800
			B	0	20	0	0	60	80	80	500	500
			C	0	0	0	0	100	100	100	500	500

Table 6 Growths on fused tin platings

SPECIMEN NO.	TYPE OF TIN	STRESS LEVEL		INSPECTION PERIOD (d) LENGTH OF WHISKERS (μm)								
				(V)3	(S)27	(S)57	(V)142	(S)181	(S)634	(S)1269	(S)5657	(S)11102
19	NORMAL Fused tin on brass substrate	HIGH	A	0	0	0	0	0	0	0	0	0
			B	0	0	0	0	0	0	0	0	0
			C	0	0	0	0	0	0	0	0	0
20	NORMAL Fused tin, copper barrier on brass	HIGH	A	0	0	0	0	0	0	0	0	0
			B	0	0	0	0	0	0	0	0	0
			C	0	0	0	0	0	0	0	0	0
39	NORMAL Fused tin on steel substrate	HIGH	A	0	0	0	0	0	0	0	0	0
			B	0	0	0	0	0	0	0	0	0
			C	0	0	0	0	0	0	0	0	0
40	NORMAL Fused tin, copper barrier on steel	HIGH	A	0	0	0	0	0	0	0	0	0
			B	0	0	0	0	0	0	6	10	0
			C	0	0	0	0	0	0	0	0	0